RECENT ADVANCES IN THE ELECTRON-PROBE MICRO-ANALYSIS OF MINERALS FOR THE LIGHT ELEMENTS

MATI RAUDSEPP

Department of Geological Sciences, The University of British Columbia, Vancouver, British Columbia V6T 1Z4

ABSTRACT

The electron-probe micro-analysis of minerals for the light elements (F, O, N, C, B and Be) is hampered by (1) absorption of the long-wavelength (>12 Å) and low-energy (<1 keV) X-radiation in the specimen and on the way to the detector, (2) low cross-sections for ionization, and (3) spectral interferences from higher-order lines of heavier elements, common in geological materials. The resulting low count-rates and generally low peak-to-background ratios place a heavy demand on the detection process, and as a consequence, the precision of the analysis. In addition, the matrix-correction programs must be substantially more robust than for the heavier elements, having to deal with large absorption-corrections, and inaccurately known mass-absorption coefficients. Other obstacles include peak shifts and changes in peak shape among chemically and structurally dissimilar specimens and standards, the availability of well-characterized standards, and beam-induced surface contamination of specimens and standards. New layered synthetic microstructures substantially increase peak count-rates, and selectively absorb some of the higher-order interferences from the heavier elements, which can hinder the measurement of peaks and background. The parallel development of layered synthetic microstructures and better matrix-correction programs during the past decade has significantly improved our capability to analyze minerals for the light elements by electron-probe micro-analysis.

Keywords: light elements, electron-probe micro-analysis, layered synthetic microstructures, wavelength-dispersion spectrometry, energy-dispersion spectrometry.

SOMMAIRE

L'utilisation de la microsonde électronique pour effectuer l'analyse de minéraux et en déterminer leurs teneurs en éléments légers (F, O, N, C, B et Be) est limitée par (1) l'absorption de la radiation X possédant une longueur d'onde supérieure à 12 Å et une faible énergie (<1 keV) par l'échantillon et au cours du parcours vers le détecteur, (2) la faible susceptibilité d'ionisation de ces éléments, et (3) les interférences spectrales dues aux raies d'ordre supérieur des éléments plus lourds, répandus dans tout matériau géologique. Il en résulte un faible taux de comptage et, en général, un faible rapport des intensités de pic et de bruit de fond, ce qui taxe le processus de détection, et, par conséquent, la précision des analyses. De plus, les logiciels servant à corriger les effets de matrice doivent être substantiellement plus robustes que pour les éléments plus lourds, vue la nécessité d'introduire les corrections importantes, et la méconnaissance des coefficients d'absorption de masse. Parmi les autres obstacles, on peut citer le déplacement des pics et le changement dans leur allure si le spécimen et l'étalon diffèrent sensiblement tant du point de vue chimique que structural, la disponibilité limitée d'étalons bien caractérisés, et la contamination de la surface des spécimens et des étalons par le faisceau. De nouvelles microstructures synthétiques en feuillets pour le choix de cristal détecteur permettent une augmentation marquée des taux de comptage, et une absorption sélective des interférences d'ordre supérieur dues aux éléments plus lourds, qui pourraient autrement nuire à la mesure des pics et du bruit de fond. Le développement parallèle de ces microstructures synthétiques en couches et de logiciels permettant une meilleure correction des effets de matrice au cours de la dernière décennie a beaucoup contribué à une capacité accrue d'analyser les minéraux pour leurs teneurs en éléments légers avec la microsonde électronique.

(Traduit par la Rédaction)

Mots-clés: éléments légers, analyse à la microsonde électronique, microstructures synthétiques en feuillet, spectrométrie en dispersion de longueurs d'onde, spectrométrie en dispersion d'énergie.

INTRODUCTION

Although macroscopic methods of X-ray spectrochemical analysis have been used routinely since their development in early part of this century, the first practical electron-probe micro-analyzer was not built until the late 1940s (Castaing 1951). Following the release of commercial instruments in the mid-1950s, electron-probe micro-analysis (EPMA) has revolutionized both the physical *and* conceptual aspects of chemical analysis in mineralogy, geology, and the other physical sciences. For the first time, miner-

alogists and petrologists could do nondestructive analysis of minerals, glasses and other geological materials (including those containing organic matter) for a wide variety of elements, with a spatial resolution of the order of a few micrometers. Characterization of variation in the chemical composition of minerals *in situ* was reduced to the microscopic scale, and the electron-probe micro-analyzer has become a cornerstone of chemical analysis in our science.

In spite of this success, a severe drawback of EPMA, until recently, was its inability to *routinely and precisely* analyze samples for the light elements (Table 1). This was because of low yields of X rays due to absorption in the specimen, the analyzer crystal and the detector window. The resulting low count-rates and generally low peak-to-background ratios place a heavy demand on the detection process. Matrix-correction programs must be substantially more robust than for the heavier elements, because of large absorption-corrections, and not very accurately known mass-absorption coefficients. Other practical obstacles include spectral interference from the higher-order lines of heavier elements, peak shifts and changes in peak shape between chemically and structurally dissimilar specimens, lack of well-characterized standards, and beam-induced surface contamination.

In the 1960s, the development of Langmuir–Blodgett type "soap" multilayer analyzers with large 2*d*-values (*e.g.*, lead stearate) for wavelength-dispersion spectrometry (Henke 1964, 1965) was the first significant advance in the analysis of samples for the light elements. An early review of this topic (Ong 1965) is an interesting account of the state of EPMA technology at that time. For the first time, the experimentally troublesome characteristic X-ray emissions of the light elements could be practically measured with wavelength-dispersion spectrometers. In the early 1980s, the diffracted intensity of X rays from light elements was dramatically improved with the introduction of layered synthetic microstructure (*e.g.*, W/Si) analyzers, which give superior reflectivity and stability compared to the stearate multilayer varieties (Nicolosi *et al.* 1986). The ability to analyze samples for light elements has improved dramatically with the availability of synthetic microstructure analyzers, improved

matrix corrections, and the development of $\phi(\rho z)$ programs.

As many common rock-forming minerals, glasses and organic components of coal and rocks contain one or more light elements as essential constituents, the compositional space accessible to mineralogists and petrologists has been significantly expanded. In addition, with the discovery of new minerals coming more often now from highly fractionated environments enriched in "incompatible" elements, the ability to analyze for the light elements has become more crucial for the proper characterization of these new phases. Although micro-analytical techniques such as the ion microprobe (Reed 1989) and single-crystal structure analysis (Hawthorne & Grice 1990) can be used for micro-analysis of materials for the light elements, and are in some cases superior in this regard, these techniques lack the spatial resolution of EPMA, require more specialized expertise, or are not as generally accessible.

A fundamental problem in the analysis of samples for the light elements (or any other element) is the acquisition of X-ray counts to a useful level of analytical precision over a practical period of time. The physics of X rays conspires against the user, and special care must be taken in all aspects of the analysis: sample preparation, data collection, selection of standards, and data reduction. In this paper, I review these general aspects, together with selected element-by-element examples from the geological and materials sciences. A review of improved data-reduction procedures with regard to the light elements and EPMA in general is beyond the scope of this paper. Thorough general reviews are given by Bastin & Heijligers (1991), Goldstein *et al.* (1992), Reed (1993) and references therein. Detailed reviews of the problems associated with specific elements (O, N, C, B) from the perspective of materials science are given in a series of papers and monographs by Bastin & Heijligers (1986a, b, d, e, 1988b, 1989b, 1990). MacKenzie (1993) reviewed electron-probe micro-analysis (including the topic of light elements) from the viewpoint of solid-state physics. Wavelength-dispersion spectrometric methods and results are discussed in more detail than energy-dispersion spectrometry (EDS), as little has been published about quantitative EDS techniques (in spite of great improvements in EDS detector technology).

IMPROVEMENTS IN HARDWARE

Wavelength-dispersion spectrometry

The development and introduction of commercially available layered synthetic microstructures (LSM, or layered dispersion elements LDE) are the most significant advances in hardware to characterize the level of concentration of light elements. Traditionally, large

TABLE 1. CHARACTERISTICS OF THE $K\alpha$ LINES OF THE LIGHT ELEMENTS

Element	Symbol	Z	λ (Å)	E (keV)
Beryllium	Be	4	114.0	0.109
Boron	B	5	67.6	0.183
Carbon	C	6	44.7	0.277
Nitrogen	N	7	31.6	0.392
Oxygen	O	8	23.62	0.525
Fluorine	F	9	18.32	0.677

(after Goldstein *et al.* 1992)

TABLE 2. SELECTED X-RAY REFLECTORS FOR THE ANALYSIS OF SAMPLES FOR THE LIGHT ELEMENTS

Name	$2d$ (Å)	Elements
TAP[1]	25.75	F
W/Si (LSM[2])	60	F, O, N
Ni/C (LSM)	95	O, N, C, B
ODPb[3] (STE)	100	O, N, C, B
Mo/B₄C (LSM)	145, 160	B, Be

[1] $C_8H_5O_4Tl$: thallium acid phtalate.
[2] Layered synthetic microstructure.
[3] $(C_{18}H_{35}O_2)_2Pb$: lead octodecanoate (lead stearate, STE).

single crystals (*e.g.*, TAP for F and O) and "soap" multilayer pseudocrystals (*e.g.*, lead stearate, for O, N, C and B) have been used to analyze the soft X-ray emissions from the light elements (Table 2). Stearate (STE) and other X-ray reflectors based on organic materials are not true crystals, being periodic in only one direction (Fig. 1). Such structures are grown by the Langmuir–Blodgett technique, in which several hundred molecular monolayers of a fatty-acid compound are deposited on a suitable substrate such as glass or mica. The fatty-acid compounds comprise a heavy atom (such as lead) and an organic tail. During deposition, the compounds are deposited layer-by-layer with the organic tail perpendicular to the surface of the substrate. The $2d$ value of the resulting

pseudocrystal depends on the length of the organic tail, and the heavy atoms behave as X-ray reflectors. Thus X-ray reflectors suitable for a variety of different ranges of wavelength can be made by adjusting the composition of the organic tail. Although the peak resolution of the stearate pseudocrystals is moderately good, they are poor X-ray reflectors, in general. In addition, they are relatively efficient transmitters of higher-order reflections of the heavier elements. Higher-order reflections of geologically important elements such as Cr, Mn, Fe, Ni, Zr, Nb and Mo may severely hamper accurate measurements of peaks and determination of background.

Table 2 lists the compositions and properties of three of the most commonly used layered synthetic microstructures. In principle, the structure of the LSM (Fig. 2) is similar to that of the conventional stearate pseudocrystals. They consist of alternating layers of light and heavy elements formed by precisely controlled deposition of vapor on an optically smooth substrate. The light-element layer controls the $2d$ value of the reflector; the "heavy" layers are the X-ray reflector. As there are many more choices of materials for the layers than for STE reflectors, LSM construction may be tailored exactly for a specific light element. Although LSM reflectors have lower resolution than corresponding STE reflectors, count rates are generally improved, and higher-order diffraction maxima from heavy elements are suppressed.
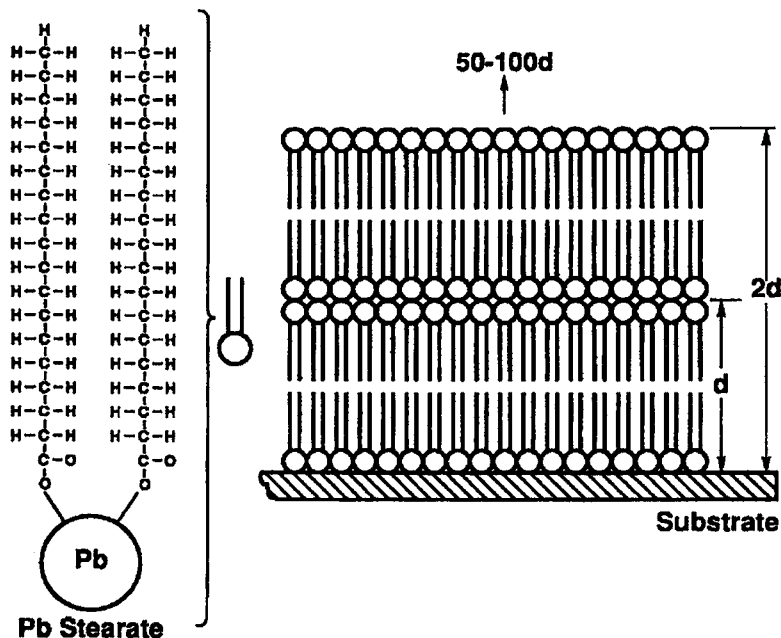

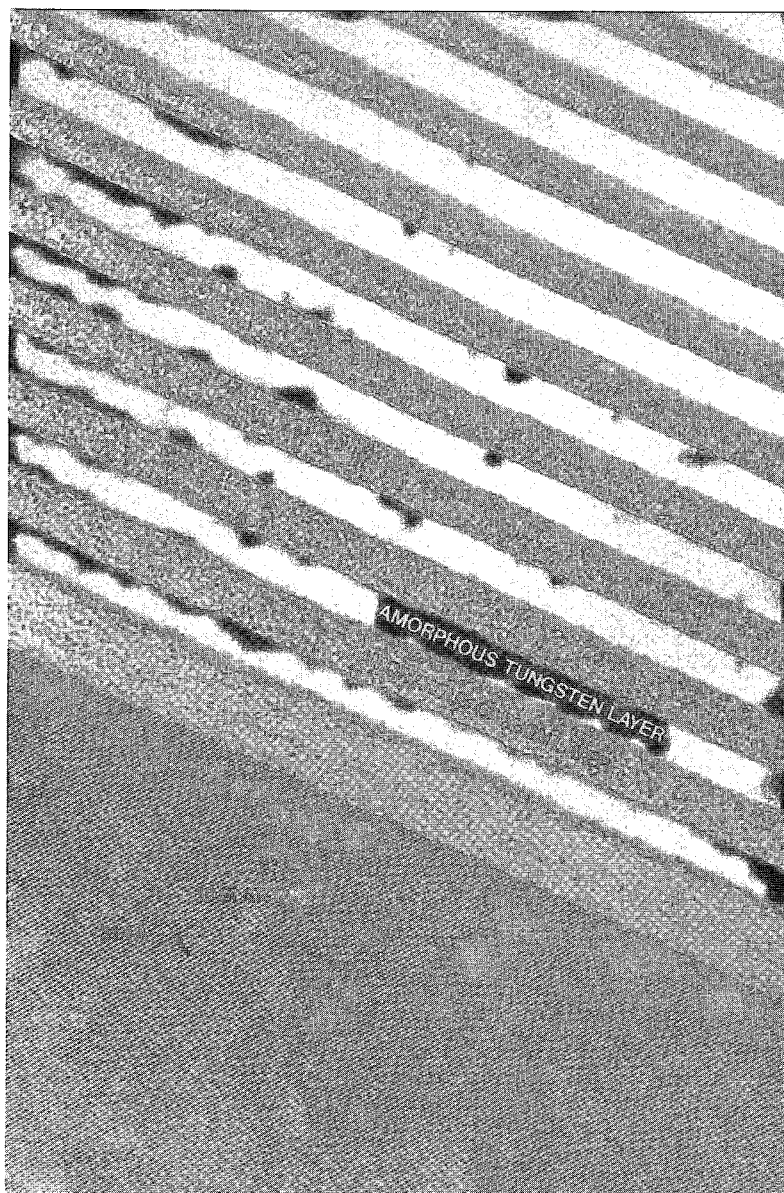FIG. 1. Lead stearate pseudocrystal grown by the Langmuir–Blodgett technique (after Goldstein *et al.* 1992).

FIG. 2. Transmission electron photomicrograph of a W/C layered synthetic microstructure ($2d$ = 64 Å). The dark and light layers are tungsten and carbon, respectively; the substrate (lower left) is a silicon wafer (courtesy of Ovonic Synthetic Materials Co. Inc.).

The performance of LSM reflectors relative to their conventional counterparts has been studied exhaustively (*e.g.*, Nicolosi *et al.* 1986, Barbee *et al.* 1986, Kawabe *et al.* 1986, 1988, Heijligers & Bastin 1986, Love & Scott 1987, Bastin & Heijligers 1986c, 1988b, 1989a, b, 1990, 1991, 1993). A good example of the significant improvement in LSM reflectors over the STE type is given by Bastin & Heijligers (1988b,

1991), who collected N$K\alpha$ spectra from eighteen nitrides. Spectra for ZrN and Zr are shown in Figure 3. Note the following differences: (i) the count rate for the N$K\alpha$ peak with the LSM is almost four times that with the STE, (ii) the peak-to-background ratio is much better with the LSM, and (iii) interferences from higher-order Zr lines are suppressed by the LSM.
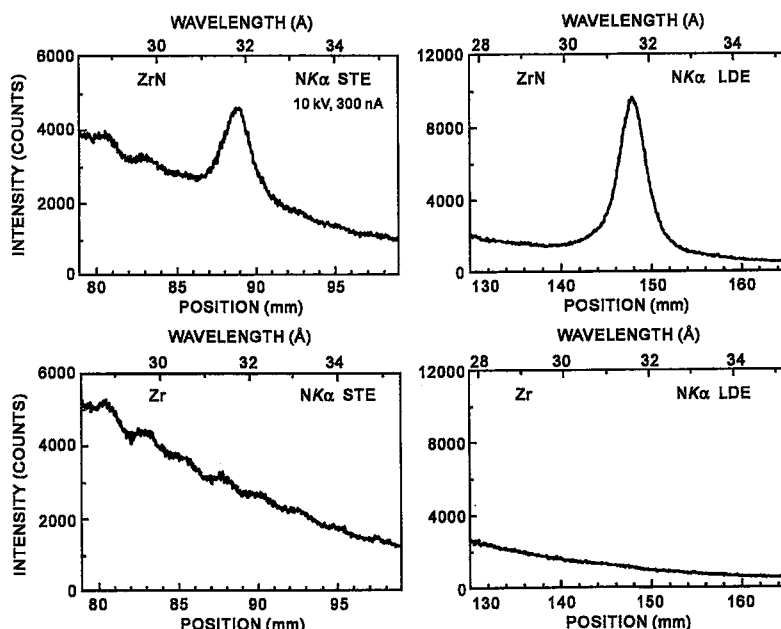
FIG. 3. Comparison of N$K\alpha$ X-ray spectra recorded from ZrN with a conventional lead stearate pseudocrystal (STE, $2d = 100$ Å) on the left and a W/Si ($2d = 60$ Å) layered microstructure (LDE) on the right. The lower half shows the backgrounds collected from Zr. Note the difference ($2 \times$) in vertical scales between STE and LDE (after Bastin & Heijligers 1991).

Excellent performance also is obtained for B$K\alpha$ with the LSM (Fig. 4). Using the LSM, the boron peak is about fifty times more intense than with the STE. Note that the spectral resolution of the LSM is less than that of the STE; however, this characteristic is a benefit, rather than a hindrance, as the LSM is thus less sensitive to peak shifts and shape changes (see below). Furthermore, this result was obtained with operating conditions similar to those used for heavier elements, an advantage as two beam currents are not required to avoid excessive dead-time corrections. An example of the sensitivity of the LSM reflectors is the detection of O$K\alpha$ from the surface of most elemental standards (Bastin & Heijligers 1991). Figure 5 shows an O$K\alpha$ peak recorded from a sample of pure gold.

In comparison with STE reflectors, the large increases in peak count-rates for boron obtained using LSM reflectors suggest that the analysis of samples for Be may be feasible. Presently, Be can be measured using the lead cerotate pseudocrystal, but with poor
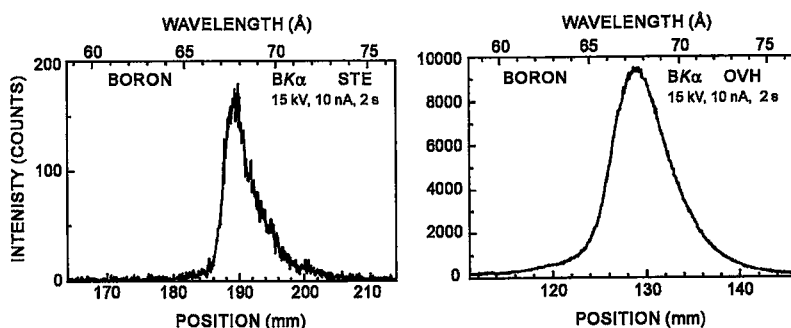

FIG. 4. Comparison B$K\alpha$ X-ray spectra recorded from elemental boron with a conventional lead stearate crystal (STE, $2d = 100$ Å) on the left and a Mo/B$_4$C layered micro-structure (OVH, $2d = 145$ Å) on the right. Note the large difference ($50 \times$) in vertical scales between STE and LDE (after Bastin & Heijligers 1991).
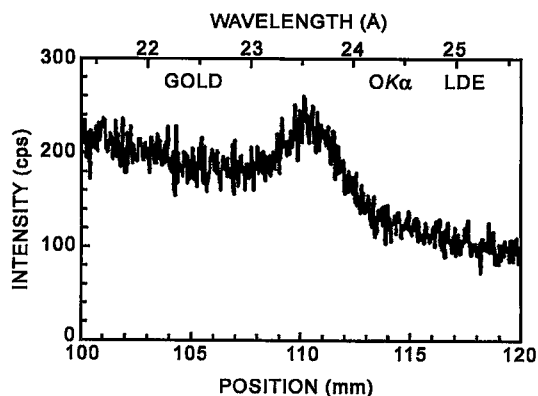
WAVELENGTH (A)

Fig. 5. O$K\alpha$ X-ray peak recorded from pure gold with a W/Si ($2d$ = 60 Å) layered microstructure: 10 kV, 50 nA (after Bastin & Heijligers 1991).

count-rates. According to Bastin & Heijligers (1991), the Mo/B$_4$C LSM gives count rates for Be$K\alpha$ twenty times higher than are obtained with the lead cerotate pseudocrystal.

Energy-dispersion spectrometry

Although significant advances have been made in energy-dispersion spectrometry (EDS), particularly in detector resolution and computer technology, the technique is still hampered by relatively poor spectral resolution and problems in processing complex overlapping spectra. On the positive side, there are no contributions from higher-order peaks, as in WDS. EDS systems are favored in industrial laboratories because they are more cost-effective than electron microprobes, are easier to use, and analysis requirements are generally less stringent than those in the research community. Virtually all scanning electron microscopes may now be equipped with sophisticated EDS systems, and one or more WDS spectrometers, but quantitative analysis of samples for the light elements with micrometer spatial resolution remains largely the realm of the electron microprobe.

In spite of the above, the development of windowless detectors and ultrathin-window (UTW) detectors now allows the *detection* of all light elements (except H, He and Li), but quantitative analysis is still only possible (with difficulty) for the heavier light elements (O, N and F). Although the UTW is slightly less sensitive than a windowless detector, it is less troublesome to maintain and is generally preferred for general-use systems. At least for now, the most useful application of light-element EDS in the geological sciences is in semiquantitative analysis and X-ray mapping (*e.g.*, Bishop *et al.* 1992). In this way, the spatial distribution of elements in relatively large areas of a specimen characterized by complex textures can be mapped

simultaneously over a few minutes to a few hours. In addition, as EDS detectors are more efficient than WDS detectors, EDS has a useful application for analyzing beam-sensitive materials, for which low beam-currents are necessary. The quantitative EDS analysis of materials for the light elements is a rapidly expanding field, and the accelerating pace of technological improvements in this area augurs well for the future.

PRACTICAL CONSIDERATIONS

Acquisition of data

The major obstacles to the acquisition of reliable low-energy X-ray intensity data are low count-rates and high absorption of the soft X-rays by the sample, the analyzer crystal, detector window and the conductive coating (usually carbon). To a large degree (depending upon the element), the development of LSM reflectors has alleviated the count-rate problem and absorption by the analyzer crystal. Recent developments in thin-window technology have reduced absorption at the detector. However, absorption in the specimen is a physical reality that can only be minimized by careful experimental technique (Goldstein *et al.* 1992): by optimization of the take-off angle to reduce X-ray absorption (shorter path in the sample), and the use of low electron-beam energies (shallow depth of X-ray production). As the take-off angle is fixed for practical purposes, the remaining variable is beam energy. Shiraiwa *et al.* (1972) showed that, for various compounds of boron, the intensity of the $K\alpha$ spectrum is a maximum between beam energies of 5 to 15 keV, depending on the sample (Fig. 6). According to Goldstein *et al.* (1992), the maximum is the result of two opposing factors: (i) X-ray intensity increases owing to increasing beam-energy and overvoltage; (ii) X-ray intensity decreases because X rays are produced deeper in the sample, and are more highly absorbed as the energy of the incident beam increases. The analysis of samples for the light elements should be done with a beam energy that gives the maximum count-rate for the peak of interest. As this is usually between 8 and 15 keV, the analysis of minerals for light elements is facilitated by this circumstance; these conditions overlap those that are normally used for some of the common heavier elements. Furthermore, if the beam energy is set too low, surface contamination produced during sample preparation and analysis, and the carbon coat, could significantly attenuate the X rays of interest. With regard to increasing count-rates by raising the beam current to high levels (100–300 nA range), Bastin & Heijligers (1991) pointed out that this could cause severe dead-time problems with the associated heavier elements, pulse-height shift problems, together with awkward experimental conditions, such as different beam-currents.
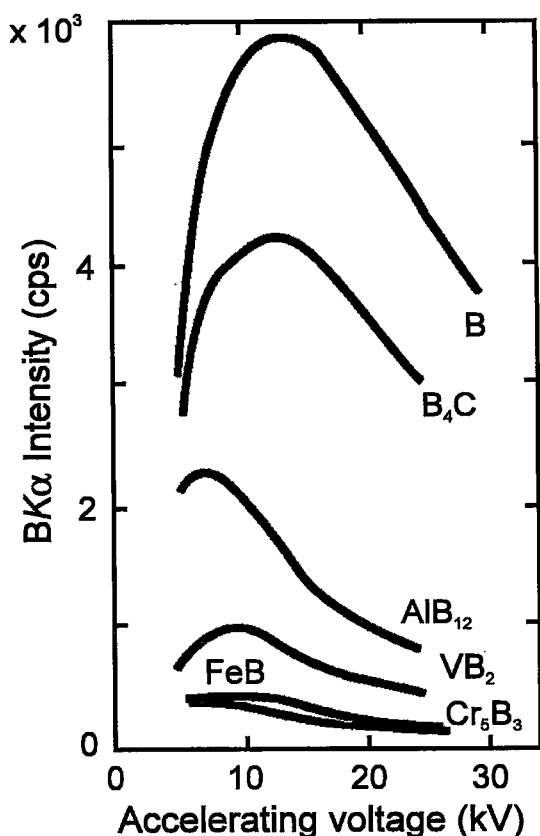
FIG. 6. $BK\alpha$ intensity *versus* accelerating voltage for boron and several of its compounds (Shiraiwa *et al.* 1972; adapted from Goldstein *et al.* 1992).

Surface contamination

The surface of a sample in contact with an electron beam gradually accumulates a layer of contamination from the interaction of the electron beam with traces of diffusion-pump oil or hydrocarbons from "dirty" samples. Such a deposit is usually manifested as a brownish ring marking the location of the beam. In the analysis of samples for heavy elements, this phenomenon is not a problem, but low-energy X-radiation emitted by the light elements can be severely absorbed by carbon in the contamination layer. In the case of carbon analysis, the effect is particularly troublesome, with $CK\alpha$ count rates increasing with time as the thickness of the contamination layer increases. The accumulation of contamination can be avoided by the installation a liquid-nitrogen-cooled cold-finger or plate close to the sample, or by directing a low-pressure jet of air onto the specimen at the point of beam incidence. Bastin & Heijligers (1988a, 1990) have

thoroughly studied these two methods of minimizing the accumulation of the contamination layer. Although cold surfaces are quite effective in reducing the contamination rate, the air-jet method is the more effective (Fig. 7), providing that the sample is not subject to oxidation. As shown by the $OK\alpha$ peak on pure gold (Fig. 5), contamination by oxygen also may be a problem if low amounts of oxygen are sought during the analysis. Goldstein *et al.* (1991) examined the effects of surface oxidation on the bulk analysis of oxygen in sensitive metals such as Ti, Zr, Hf, and their alloys. As these oxide layers cannot be removed, their influence on the measured bulk-concentration of oxygen must be known. Although such oxidation of most silicates and oxides is unlikely, it could be significant in certain sulfides and metals. Bastin & Heijligers (1988a, 1990) pointed out that the rate of beam-induced contamination is not predictable, but varies from day to day, depending on the state of the instrument and sample. Also, contamination effects may differ substantially; for example, good conductors of heat such as Cu are contaminated easily, whereas insulators, such as Si and B, show low rates of contamination. In view of these findings, it is unlikely that beam-induced contamination by carbon and oxygen on the surface of typical geological specimens is a severe problem, as major amounts of these elements are generally present in the sample. However, if small differences in the concentrations of these elements are to be determined, the analyst must take this possibility into account.

Conducting layers

As most geological samples to be analyzed by EPMA are insulators, the surface of the sample must be coated with a conducting layer, usually carbon, to a thickness of about 200 Å. Such a layer is essentially
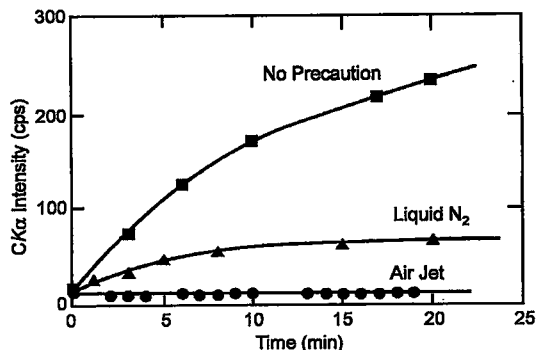

FIG. 7. Effect of anticontamination devices on carbon-contamination rate on polished copper: 10 kV, 100 nA, stearate crystal, oil-diffusion-pumped system (after Bastin & Heijligers 1990).

another form of surface contamination, and the problems with regard to the absorption of soft X rays are the same as those described in the previous section. Armstrong (1993) showed that the variation in carbon-coat thickness between sample and standard can result in systematic errors of greater than 1%. In the case of a sample of SiO_2, a variation of carbon-coat thickness of 100 Å causes the $OK\alpha$ intensity to vary by about 3.8% at an accelerating voltage of 15 kV. Test mounts 2.5 cm across were placed symmetrically and at a constant distance from the carbon electrodes, and spun symmetrically with respect to the electrodes during evaporation. The variation in a nominal carbon-coat thickness of 200 Å was about 5 to 10 Å for adjacent specimens, but up to 40 to 50 Å across the whole mount. Indeed, localized patches varying in thickness by 100 Å were observed. In spite of careful carbon-coating procedures, Armstrong (1993) showed that variations in the coat thickness may still produce analytical errors at the 1% level. Although the effects of variation in carbon-coat thickness can be corrected for using current $\phi(\rho z)$ models (e.g., Pouchou & Pichoir 1991) and thin-film data-reduction programs (e.g., Waldo 1991), accurate analysis of samples for the light elements requires that standards and samples be carbon-coated at the same time in adjacent mounts with careful attention to technique.

Chemical shifts and peak-shape alterations

In the electron-probe micro-analysis of samples for the heavy elements by WDS, the usual experimental method is to acquire intensity data for X-ray peaks from standards and samples at predetermined positions of intensity maxima. As Bastin & Heijligers (1991) emphasized, this procedure works only if the intensity of a peak is proportional to its integrated intensity, as it is for K and L radiation from elements of medium to high atomic number. However, for light elements, this assumption fails not only because peak positions may shift from sample to sample, but also because the peak shapes may be quite different. These changes in peak position and peak shape occur because the K emission of the light elements involves valence electrons and is thus affected by the local bonding environment of the atom.

The possible magnitude of the bonding effect can be seen by comparing the $CK\alpha$ peaks from glassy carbon and TiC (Bastin & Heijligers 1991). In Figure 8, the net intensities of the peaks are scaled to the same value (peak k-ratio = 1), but note that the peak from glassy carbon is about twice as wide as that from TiC, and that the peak positions do not exactly coincide. Although the peak shift could be corrected for by simply repositioning the spectrometer, the peak-shape difference still would result in an error of about 50%.

The situation for boron is even more complicated. In addition to the expected peak-shifts and changes in
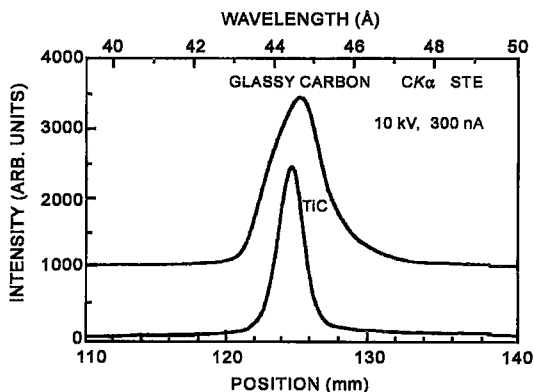

FIG. 8. $CK\alpha$ peaks recorded from glassy carbon and TiC with stearate crystal. Peaks are scaled to the same net count-rates (after Bastin & Heijligers 1991).

shape, there are further effects (Bastin & Heijligers 1991): (i) the peak position can depend strongly on the crystallographic orientation of a particular sample; (ii) the peak shape varies synchronously with the peak shifts. Figure 9 shows two extremes in peak shift and shape change for $BK\alpha$ peaks recorded with two extreme orientations of crystals of ZrB_2. The synchronous changes in peak intensity reflect the presence of polarized components (Wiech 1981) in the emitted radiation, together with some filtering action by the lead stearate crystal. In this regard, the behavior of $BK\alpha$ radiation is similar to that of light passing through a crystal between crossed polarizers. Although the polarization of X rays is theoretically possible in all non-cubic borides, Bastin & Heijligers (1991) noted that about 50% of 28 non-cubic borides (including elemental boron) studied do not show measurable peak-shifts. However, large differences in peak shape are present.
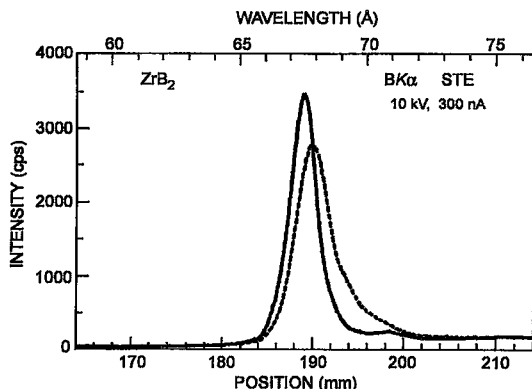

FIG. 9. Extremes in $BK\alpha$ peak intensities recorded from ZrB_2 with stearate crystal (after Bastin & Heijligers 1991).

In summary, if peak shifts and shape changes are ignored, large errors in data acquisition may occur during analysis of samples for the light elements. Intensity data must be acquired with time-consuming methods of integration. According to Bastin & Heijligers (1991), the effect depends on atomic number, being most severe for boron, slightly less for carbon (polarization effects absent), and least severe for nitrogen, oxygen and fluorine.

Selection of standards

With the development of increasingly more robust programs of quantification, the necessity of using standards very similar in composition to that of the sample has become progressively less important than in the past for *routine* electron-probe micro-analysis. However, in view of the preceding discussion, selection of appropriate standards is absolutely crucial for the analysis of samples for light elements. Notable concerns are uncertainties in mass-absorption coefficients and composition-dependent peak shifts and changes in peak shape. In the case of non-cubic boron compounds, documentation of crystallographic orientation also is necessary. Thus accurate results can best be obtained by using well-characterized standards similar in composition (and orientation where necessary), thereby reducing the magnitude of the matrix correction.

McGuire *et al.* (1992) have rigorously evaluated 13 minerals as standards for oxygen. They selected a range of compositions and structures that are representative of most minerals, are homogeneous and free of inclusions. These samples were analyzed for heavy elements by electron microprobe and X-ray fluorescence (XRF), for oxygen using fast-neutron activation analysis (FNAA), for hydrogen (hydrous samples) by U extraction, and for $Fe^{3+}/\Sigma Fe$ by Mössbauer spectro-
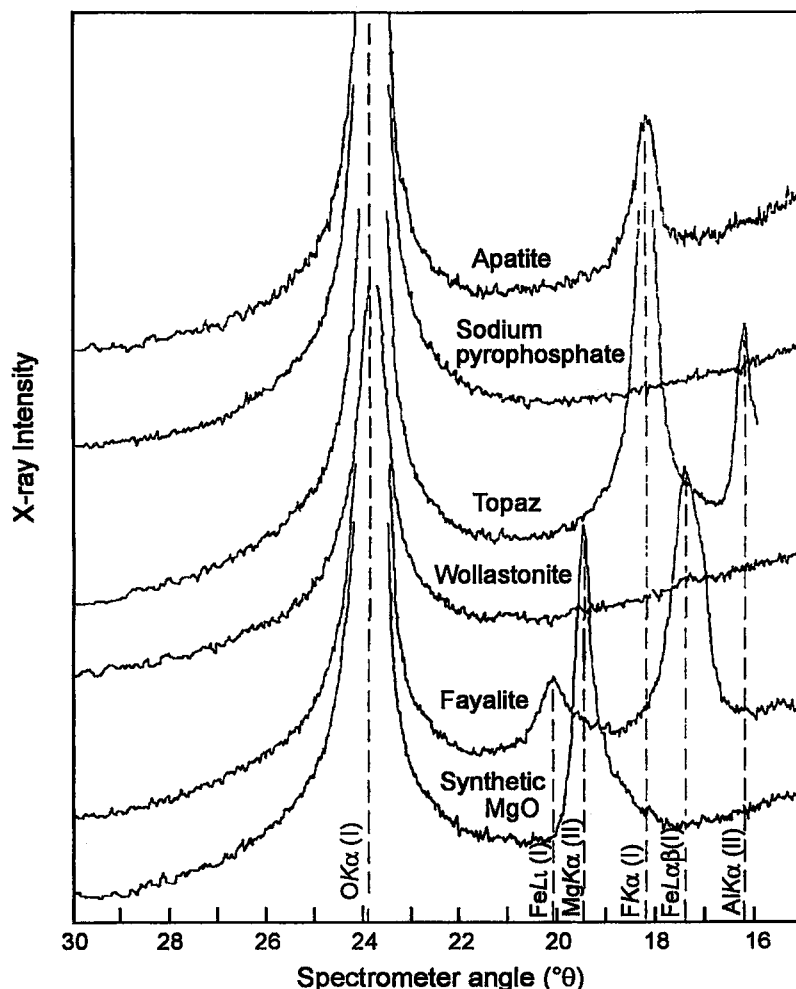

FIG. 10. Spectral scan using a W/Si ($2d = 60$ Å) LSM in the region of the $FK\alpha$ peak on selected samples (after Potts & Tindle 1989).

scopy. The majority of samples are stoichiometric in oxygen, but enstatite, muscovite and biotite apparently contain more oxygen than expected. McGuire *et al.* (1992) pointed out that in view of their results, it is dangerous to assume that minerals will have stoichiometric proportions of oxygen. This collection of standards is available to the electron-probe micro-analysis community and should provide a good starting point for the determination of oxygen. I have begun testing these standards in my laboratory, and so far have obtained excellent results (Raudsepp, unpubl. data).

ANALYSIS OF MINERALS FOR THE LIGHT ELEMENTS: EXAMPLES

Fluorine

Although fluorine is the heaviest of the light elements, it has been well known for some time that the FKα peak shows considerable variation in peak position and shape from mineral to mineral (*e.g.*, Solberg 1982). Other complicating factors are low count-rates with TAP crystals, and interference from the third-order PKα peak in phosphates.

The new LSM reflectors have improved the state of fluorine EPMA considerably. Potts & Tindle (1989) reported up to 14 times the FKα count-rate using a W/Si ($2d = 60$ Å) LSM, compared to that obtained with a TAP crystal. In addition, multiple-order interferences greater than second order are absent; this is particularly good news for the analysis of apatite for fluorine, as the third-order PKα peak is absent. Detection limits are two to three times better than those from TAP measurements. Spectral scans in the region of the FKα peak (Fig. 10) show the absence of higher-order interferences from heavy elements. However, note that second-order peaks from Mg and Al, and first-order *L*-lines from Fe, offer potential interferences. These interferences are not a problem in the analysis of apatite and many other fluorine-bearing minerals, but the determination of fluorine in minerals rich in Mg, Al and transition metals is not straightforward with the LSM.

Apparent mobility of fluorine ions in apatite under beam conditions routinely used for mineral analysis (15 kV, 15 nA) has recently been described by Stormer *et al.* (1993) in a study of the variation of FKα (and ClKα) intensity in apatite. According to the results of their study, fluorine ions apparently diffuse to the surface under the influence of the electric field produced by the primary-beam electrons in the analytical volume. Furthermore, the degree of diffusion depends on the crystallographic orientation of the apatite crystal. The magnitude of this effect is clearly shown in Figure 11, a comparison of FKα intensity *versus* total cumulative beam-exposure time for apatite, topaz and fluorite. Figure 11A shows that on the (001) section of apatite, the FKα intensity increases by a factor of two
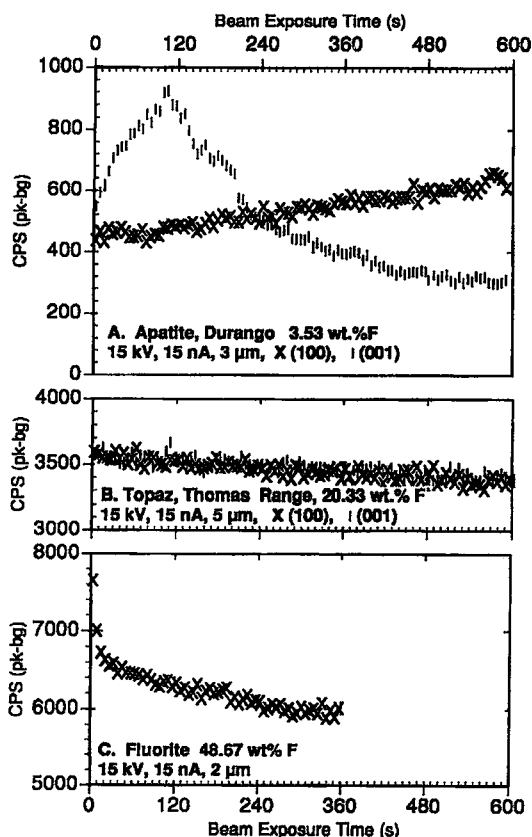

FIG. 11. FKα X-ray intensity variation *versus* orientation. FKα X-ray intensity plotted against total cumulative beam-exposure time for (A) (001) and (100) sections of fluorapatite, (B) (001) and (100) sections of topaz, and (C) a section of fluorite of unknown orientation. Data were obtained during 6-s count intervals separated by 3 s of beam blanking (after Stormer *et al.* 1993).

during the first 60–120 s, followed by a decline over the next 340 s, and then approaches a constant value below the initial value. On (100) sections of apatite, the intensity increases about 20% over the same period. In contrast to apatite, the FKα intensity on topaz is nearly constant for both orientations (Fig. 11B), declining about 5% (probably owing to surface contamination). On fluorite (Fig. 11C), the intensity of FKα decreases at least 20% in the first 60 s. According to Stormer *et al.* (1993), fluorine-bearing amphiboles and micas do not show this type of behavior. Figure 12 shows that the effect is actually qualitatively similar on both sections of apatite if the time scale for the (100) section is compressed. In summary, Stormer *et al.* (1993) concluded that (i) the variation of FKα intensity during analysis of apatite is large enough to cause significant analytical errors, particularly as the effect is orienta-
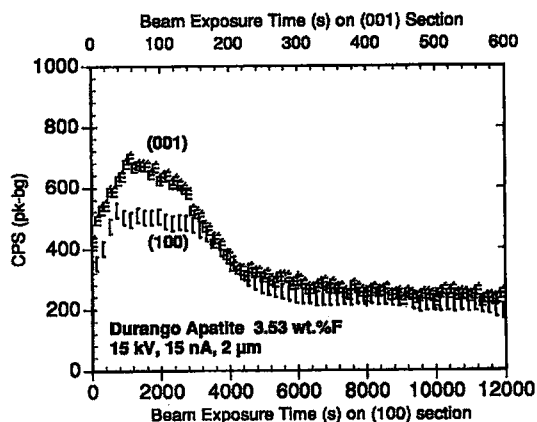
FIG. 12. Comparison of time scales of variation in F$K\alpha$ X-ray intensity on (100) and (001) sections of fluorapatite. F$K\alpha$ X-ray intensity plotted against total cumulative beam-exposure time for (001) (6-s count interval) and (100) (200-s count interval) sections of fluorapatite. Beam-blocking intervals were 3 s for both sections. Note the time-scale compression (20 ×) for the (100) section (lower x axis) (after Stormer et al. 1993).

tion-dependent; (ii) reduction of the beam current reduces the variation in intensity, but degrades the overall intensity and thus analytical precision; (iii) the analysis of apatite for fluorine is best done by doing multiple analyses on the same spot and using cumulative beam-exposure time, and extrapolating back to the initial count-rate; (iv) apatite should not be used as a standard if beam-exposure history is not controlled; (v) if integrated peak-areas are used together with a suitable matrix-correction program, topaz can be used as a standard for fluorine.

Oxygen

As oxygen is the most abundant element in the Earth's crust, the capability of analyzing minerals for oxygen accurately and precisely is of significant importance. It is not normally sought in mineralogical studies; instead, its concentration has been inferred from considerations of stoichiometry. Such calculations are useful for minerals in which all of the cations and other anions have been determined, but cannot account for the oxygen associated with unmeasured cations, especially the other light elements, H, Li, Be, B, C and N. In addition, the quality of the analytical results is difficult to assess if the valence state of all of the cations (notably iron) is not known. Other geological materials, such as natural glass, are even more problematical, as there is no recourse to stoichiometry. Furthermore, as variable amounts of volatiles and the problem of alkali-cation migration in glass are an additional concern to the analyst, their direct analysis for oxygen gives more confidence in the results.

With the development of LSM reflectors, the capability to analyze for oxygen has improved dramatically. In particular, the W/Si ($2d = 60$ Å) gives optimum results for oxygen, and has the additional benefit of being a good detector for fluorine and nitrogen also. In a study of a variety of oxide and silicate minerals, Armstrong (1988) noted that O$K\alpha$ peak-shapes are similar in different compounds, but not identical. Measured differences in the ratio of the peak height to the net area of the peak were 3% more for MgO than for Al_2O_3 (the primary standard), about 4% less for SiO_2 than for Al_2O_3, and about 13.5% less for TiO_2 than SiO_2. These differences must be corrected for in the data-reduction routine; the symmetrical, near-Gaussian shape of the peaks from the W/Si reflector makes peak fitting, background subtraction and peak integration relatively easy (Armstrong 1988). In summary, Armstrong (1988) concluded that *with care* in carbon coating, in avoiding surface contamination and in the correction procedure used, quantitative analysis for oxygen with a W/Si LSM can be done with a degree of accuracy and precision approaching that of the other major elements.

Nash (1992) reported the levels of concentration of oxygen in various mineral standards, hydrous minerals and samples of natural glass. The analyses were done using the W/Si LSM with an accelerating voltage of 15 kV, a beam current of 25 nA, a beam size between 5 and 25 μm, and a counting time of 20 s. Relative intensities of the peaks were used, together with the $\phi(\rho z)$ algorithm of Pouchou & Pichoir (1991), and with mass-absorption coefficients from Henke et al. (1982). Figure 13 shows the nominal oxygen content (assum-
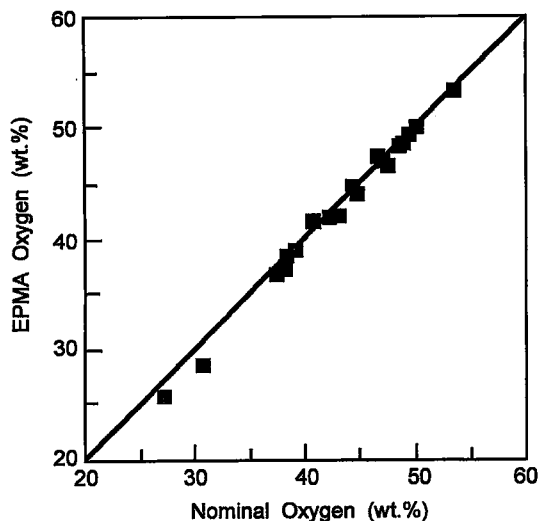

FIG. 13. Comparison of measured content of oxygen with nominal content (assuming stoichiometry) in a variety of mineral standards. The analytical error is less than the size of the data points (after Nash 1992).

ing stoichiometry) *versus* the measured values in 18 minerals. Synthetic Al_2O_3 was used as the primary standard. In general, the correlation between measured and nominal amounts of oxygen is good, but hematite and magnetite have measured oxygen contents that are low by about 1% absolute (two lowest points, Fig. 13). Nash (1992) attributed this discrepancy to peak-shape differences between Al_2O_3 and the iron oxides. His determinations for hornblende and N-bearing illite gave analytical totals of 99.8 and 99.4%, respectively. For the illite, the concentration of nitrogen also was measured (see below). According to Nash (1992), the analysis of minerals for oxygen gives confidence in the quality of the analysis for the cations (from the analytical total), and if the valence states of the cations is known, the concentration of hydrogen can be estimated.

Nash (1992) also used direct analysis of natural glasses for oxygen in order to *estimate* the H_2O content by difference, with the additional advantage of monitoring the quality of the analyses from the analytical totals. The concentration of oxygen was determined with a precision of 0.6% of the amount present. He pointed out that the method is not as precise (about 1% absolute for H_2O) as infrared spectroscopy, and cannot measure H directly, but it is simple, and the result can be obtained during any analysis in which oxygen is measured. Figure 14 shows estimates of H_2O contents (from EPMA) of samples of silicic glass compared

with H_2O measured by secondary ion mass spectrometry (SIMS) and manometry. The EPMA concentrations agree (within the level of precision) with the results from both manometry and SIMS, but the results from SIMS show more scatter (*i.e.*, are less precise).

Nitrogen

Nitrogen is a particularly troublesome element to analyze for with the electron microprobe (Bastin & Heijligers 1988b), because of extremely low peak-to-background ratios, curved background, and the many higher-order interferences from Zr, Nb and Mo if STE reflectors are used. Using the new W/Si reflector ($2d = 60$ Å) increases count rates and peak-to-background ratios, and eliminates the higher-order interferences. However, interference of the Ti*Ll* peak with the N*Kα* peak is still potentially serious in Ti-bearing compounds.

NH_4-bearing silicates (*e.g.*, tobelite, buddingtonite, ammonioalunite) are common in many hydrothermal environments associated with the alteration of black shales, rhyolites and andesites. Wilson *et al.* (1992) demonstrated the effectiveness of the W/Si LSM in a study of tobelite-bearing veins from black shale. They measured the N and O contents of NH_4-bearing silicates directly by EPMA, using conditions similar to those of Nash (1992). AlN was used as the standard for N. As the Ti contents in these samples are negligible, interference with the N*Kα* peak was ignored.

Carbon

As has been shown (Fig. 8), the C*Kα* peak is subject to severe alteration in shape and shifts in position from bonding effects. As a consequence, errors of 30–50% can result if these effects are neglected when using the STE reflector. If an LSM is used, the inherently poorer resolution of these devices reduces this error to about 15% or more. In spite of these practical problems, EPMA of samples for carbon (together with oxygen and nitrogen) using a Ni/C LSM ($2d = 95$ Å) has been applied extensively to coal studies with good success (Bustin *et al.* 1993, Mastalerz & Bustin 1993a, b, Mastalerz *et al.* 1993a, b). To avoid damage to the sample, a beam size of 10 μm, an accelerating voltage of 10 kV, and beam current of 10 nA were used. As only coal of high rank (greater than semianthracite) is a good electrical conductor, 230 Å of carbon was coated on all samples. To avoid changes in peak shape and shifts of peaks, anthracite was used as the primary standard for carbon, being close to the samples in composition. Extensive studies by these investigators show neither peak shifts or changes in shape between the standard and unknowns. The results for carbon and oxygen show excellent agreement (within experimental error) with results from the ASTM method (by combustion).
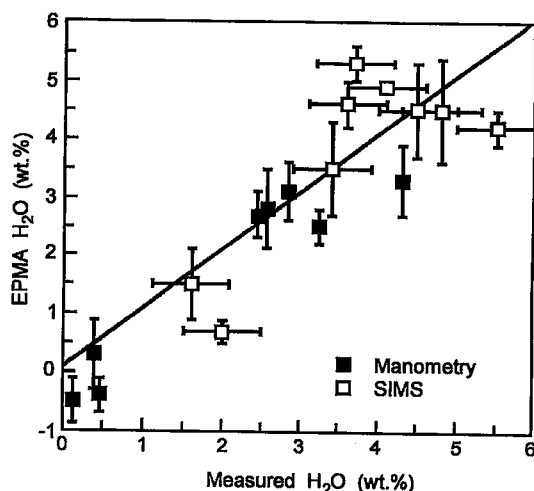

FIG. 14. H_2O content of hydrated glass estimated from EPMA *versus* H_2O content determined by secondary-ion mass spectrometry (SIMS) on melt inclusions (open squares) and by manometry on obsidian glass separates (solid squares), after Nash (1992). The line is the linear least-squares fit to the data. The error bars on the EPMA values are standard deviations for ten analyses on each sample. SIMS error estimates are 0.5%; manometry uncertainties are less than the size of the data points.

TABLE 3. EXPERIMENTAL CONDITIONS AND BORON COUNT DATA USING Mo/B$_4$C LSM

Material	B (wt.%)	Voltage (kV)	Current (nA)	Peak (cps)	Bkgd (cps)	(P-B)/B[*]	MDL[**] (wt.%)
LaB$_6$†	31.8	10	15	9800	50	195	0.01
SRM-93A†	3.9	10	15	80	13	5.2	0.1
SRM-93A‡	3.9	15	46	130	23	4.6	0.1
SRM-93A†	3.9	15	28	65	10	5.5	0.1
SRM-93A†	3.9	15	18	55	8	5.8	0.1

(after McGee et al. 1991)

[*] Ratio of background-corrected peak counts to background counts.
[**] MDL% = estimated minimum detection limit, in wt.% B, for count times of 30 s.
† Mo/B$_4$C ($2d$ = 163 Å)
‡ Mo/B$_4$C ($2d$ = 148 Å)

Boron

As X-ray emissions from boron show not only large peak-shifts and changes in peak shape (*e.g.*, Fig. 9), but also are dependent on crystallographic orientation in many relatively simple non-cubic boron compounds, one may expect that such variations will be important in minerals. McGee et al. (1991) presented results of an EPMA study of boron distribution in minerals using two different Mo/B$_4$C reflectors ($2d$ = 143, 163 Å), and found no significant variation in peak shift or in peak shape between a standard borosilicate glass (NIST, SRM–93A, 12.5% B$_2$O$_3$) and tourmaline and biotite (although they admit that peak shapes were not rigorously evaluated). A potential problem uncovered in this study is the interference of the ClL_4 and ClL_n peaks at 67.9 and 67.33 Å, respectively, with the B$K\alpha$ peak at 67.6 Å. If these overlaps are not accounted for, errors in measurement of intensity of the B peak of about 1 to 2 times the amount of Cl present may result. As these interferences are from first-order peaks, empirical corrections must be made based on compositions of boron-free, chlorine-bearing standards. The analytical conditions used and typical intensities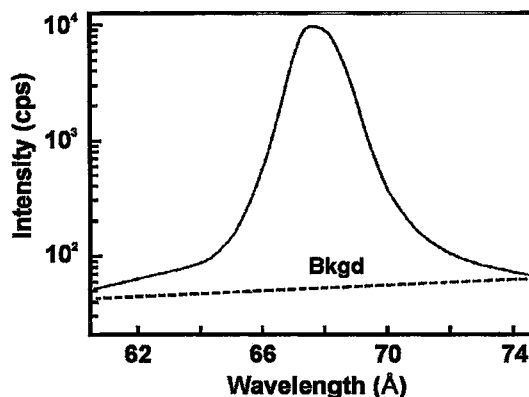 of B peaks are given in Table 3. As the B$K\alpha$ peak (Fig. 15) is broad (FWHM = 0.8 Å), background must be measured 6–10 Å on either side of the peak. However, to shorten the duration of the analysis, McGee et al. (1991) calculated the backgrounds for the sample by measuring the background counts as a function of average atomic number for the standards, and calculating backgrounds for the samples by interpolation. Although less accurate than actual measurement, this procedure has the advantage of minimizing beam-induced surface contamination and migration of elements. Data reduction was done using the correction procedures of Bence & Albee (1968). McGee et al. (1991) concluded that: (i) the electron-probe micro-analysis of samples for boron can be routinely done in tourmaline and other boron-rich minerals, and (ii) minor contents of boron can be determined with approximate limits of detection of 0.3 wt.% B$_2$O$_3$ for counting times of 3–5 minutes.

Beryllium

The prospect of analyzing quantitatively for beryllium in minerals is presently dim. In spite of successes in the *detection* of beryllium in simple binary alloys using a Mo/B$_4$C LSM ($2d$ = 198 Å) (*e.g.*, Sentner & Heitur 1987, Kawabe et al. 1988), count rates even on elemental beryllium are low. Furthermore, in view of the peak shift, changes in peak shape and crystallographically dependent behavior of X-ray emission in boron, similar (or worse) behavior in beryllium is quite likely.

CONCLUSIONS

In the thirty-year period since the review of electron-probe micro-analysis of solids for light elements by Ong (1965), this aspect of EPMA has undergone revolutionary changes, particularly with respect to the development and testing of layered synthetic microstructures as X-ray reflectors, detailed documentation of the nature of X-ray emission from light elements in a wide variety of simple compounds and minerals, and greatly improved data-reduction programs. The most significant improvements have

FIG. 15. B$K\alpha$ peak from LaB$_6$ (31.8 wt.% B) at 10 kV accelerating voltage and 15 nA sample current, using Mo/B$_4$C ($2d$ = 163 Å) LSM (after McGee et al. 1991).

occurred in wavelength-dispersion methods, but recent advances in energy-dispersion spectrometry show great promise for the near future. We can now analyze materials for elements as light as boron with a high degree of confidence in the results, and can detect beryllium. Although techniques such as SIMS can more successfully determine concentrations of the light elements beyond the reach of EPMA (Be, Li, H), the greater accessibility and convenience of the electron-probe micro-analyzer ensure that it will play an important role in micro-*in situ* analysis of Earth materials for the light elements in the years ahead.

REFERENCES

ARMSTRONG, J.T. (1988): Accurate quantitative analysis of oxygen and nitrogen with a W/Si multilayer crystal. *In* Microbeam Analysis (D.E. Newbury, ed.). San Francisco Press, Inc., San Francisco, California (301-304).

————— (1993): Effects of carbon coat thickness and contamination on quantitative analysis: a new look at an old problem. *Microbeam Analysis* 2, Supplement (J.T. Armstrong & J.R. Porter, eds.). VCH Publishers, Inc., Deerfield Beach, Florida (S13-S14).

BARBEE, T., BLEU, D.J., VON ROSENSTIEL, A.P., KNIPPENBERG, W., HUIZING, A. & WILLICH, P. (1986): LSM X-ray reflection crystals for light element analysis in electron microprobes. *In* 11th Int. Congress on X-ray Optics and Microanalysis (J.D. Brown & R.H. Packwood, eds.). ICXOM, London, Ontario (520-522).

BASTIN, G.F. & HEIJLIGERS, H.J.M. (1986a): Quantitative electron probe microanalysis of carbon in binary carbides. I. Principles and procedures. *X-ray Spectrom.* 15, 135-142.

————— & ————— (1986b): Quantitative electron probe microanalysis of carbon in binary carbides. II. Data reduction and comparison of programs. *X-ray Spectrom.* 15, 143-150.

————— & ————— (1986c): Recent developments in EPMA of very light elements. *In* 11th Int. Congress on X-ray Optics and Microanalysis (J.D. Brown & R.H. Packwood, eds.). ICXOM, London, Ontario (257-261).

————— & ————— (1986d): Quantitative electron-probe microanalysis of boron in some binary borides. *In* Microbeam Analysis (A.D. Romig, Jr. & W.F. Chambers, eds.). San Francisco Press, Inc., San Francisco, California (285-288).

————— & ————— (1986e): Quantitative electron probe microanalysis of boron in binary borides. Internal Rep., Eindhoven Univ. of Technology, Eindhoven, The Netherlands.

————— & ————— (1988a): Contamination phenomena in the electron probe microanalyzer. *In* Microbeam Analysis (D.E. Newbury, ed.). San Francisco Press, Inc., San Francisco, California (325-328).

————— & ————— (1988b): Quantitative electron probe microanalysis of nitrogen. Internal Rep., Eindhoven Univ. of Technology, Eindhoven, The Netherlands.

————— & ————— (1989a): Quantitative EPMA of oxygen. *In* Microbeam Analysis (P.E. Russell, ed.). San Francisco Press, Inc., San Francisco, California (207-210).

————— & ————— (1989b): Quantitative electron probe microanalysis of oxygen. Internal Rep., Eindhoven Univ. of Technology, Eindhoven, The Netherlands.

————— & ————— (1990): Quantitative electron probe microanalysis of carbon in binary carbides (3rd ed.). Internal Rep., Eindhoven Univ. of Technology, Eindhoven, The Netherlands.

————— & ————— (1991): Quantitative electron probe microanalysis of ultra-light elements (boron-oxygen). *In* Electron Probe Quantitation (K.F.J. Heinrich & D.E. Newbury, eds.). Plenum Press, New York, N.Y. (145-161).

————— & ————— (1993): Synthetic multilayer crystals for EPMA of ultra-light elements. *Microbeam Analysis* 2, Supplement (J.T. Armstrong & J.R. Porter, eds.). VCH Publishers, Inc., Deerfield Beach, Florida (S188-S189).

BENCE, A.E. & ALBEE, A.L. (1968): Empirical correction factors for the electron microanalysis of silicates and oxides. *J. Geol.* 76, 382-403.

BISHOP, A.N., KEARSLEY, A.T. & PATIENCE, R.L. (1992): Analysis of sedimentary organic materials by scanning electron microscopy: the application of backscattered electron imagery and light element microanalysis. *Org. Geochem.* 18, 431-446.

BUSTIN, R.M., MASTALERZ, M. & WILKS, K.R. (1993): Direct determination of carbon, oxygen and nitrogen content in coal using the electron microprobe. *Fuel* 72, 181-185.

CASTAING, R. (1951): *Application des Sondes Électroniques à une Méthode d'Analyse Ponctuelle Chimique et Cristallographique.* Thèse de doctorat, Université de Paris, Paris, France.

GOLDSTEIN, J.J., CHOI, S.K., VAN LOO, F.J.J., HEIJLIGERS, H.J.M., DIJKSTRA, J.M. & BASTIN, G.F. (1991): The influence of surface oxygen contamination of bulk EPMA of oxygen in ternary titanium–oxygen-compounds. *In* Microbeam Analysis (D.G. Howitt, ed.). San Francisco Press, Inc., San Francisco, California (57-58).

————, NEWBURY, D.E., ECHLIN, P., JOY, D.C., ROMIG, A.D., LYMAN, C.E., FIORI, C. & LIFSHIN, E. (1992): *Scanning Electron Microscopy and X-ray Microanalysis* (2nd ed.). Plenum Press, New York, N.Y.

HAWTHORNE, F.C. & GRICE, J.D. (1990): Crystal-structure analysis as a chemical analytical method: application to light elements. *Can. Mineral.* **28**, 693-702.

HEIJLIGERS, H. & BASTIN, G. (1986): The performance of an "LSM" crystal compared to that of a conventional stearate crystal for the quantitative EPMA of nitrogen. *Beitr. Elektronenmikroskop. Direktabb. Oberfl.* **19**, 1-6.

HENKE, B.L. (1964): X-ray fluorescence analysis for sodium, fluorine, oxygen, nitrogen, carbon, and boron. *In* Advances in X-ray Analysis 7 (W.M. Mueller, G.R. Mallet & M.J. Fay, eds.). Plenum Press, New York, N.Y. (460-488).

———— (1965): Some notes on ultrasoft X-ray fluorescence analysis – 10 to 100 Å region. *In* Advances in X-ray Analysis **8**. Plenum Press, New York, N.Y. (260-284).

————, LEE, P., TANAKA, T.J., SHIMABUKURO, R.L. & FUJIKAWA, B.K. (1982): Low-energy X-ray interaction coefficients: photoabsorption, scattering, and reflection. *Atomic Data and Nuclear Data Tables* **27**, 1-144.

KAWABE, K., SAITO, M., KATO, A., TOMITA, T. & TAGATA, S. (1986): Coated multilayer dispersion element for X-ray microanalysis. *In* Proc. XIth Int. Congress on Electron Microscopy (Kyoto), 569-570.

————, TAKAGI, S., SAITO, M. & TAGATA, S. (1988): Layered synthetic microstructure dispersion elements for electron probe microanalysis of carbon, boron and beryllium. *In* Microbeam Analysis (D.E. Newbury, ed.). San Francisco Press, Inc., San Francisco, California (341-344).

LOVE, G. & SCOTT, V.D. (1987): Progress in the EPMA of light elements. *Inst. Phys., Conf. Ser.* **90**, 349-352.

MACKENZIE, A.P. (1993): Recent progress in electron probe microanalysis. *Rep. Prog. Phys.* **56**, 557-604.

MASTALERZ, M. & BUSTIN, R.M. (1993a): Variation in elemental composition of macerals; an example of the application of electron microprobe to coal studies. *Int. J. Coal Geol.* **22**, 83-99.

———— & ———— (1993b): Variation in maceral chemistry within and between coals of varying rank: an electron microprobe and micro-Fourier transform infra-red investigation. *J. Microscopy* **171**, 153-166.

————, ———— & LAMBERSON, M.N. (1993a): Variation in chemistry of vitrinite and semifusinite as a function of associated inertinite content. *Int. J. Coal Geol.* **22**, 149-162.

————, WILKS, K.R. & BUSTIN, R.M. (1993b): Variation in vitinite chemistry as a function of associated liptinite content; a microprobe and FT-i.r. investigation. *Org. Geochem.* **20**, 555-562.

MCGEE, J.J., SLACK, J.F. & HERRINGTON, C.R. (1991): Boron analysis by electron microprobe using MoB_4C layered synthetic crystals. *Am. Mineral.* **76**, 681-684.

MCGUIRE, A.V., FRANCIS, C.A. & DYAR, M.D. (1992): Mineral standards for electron microprobe analysis of oxygen. *Am. Mineral.* **77**, 1087-1091.

NASH, W.P. (1992): Analysis of oxygen with the electron microprobe: applications to hydrated glass and minerals. *Am. Mineral.* **77**, 453-457.

NICOLOSI, J.A., GROVEN, J.P., MERLO, D. & JENKINS, R. (1986): Layered synthetic microstructures for long wavelength X-ray spectrometry. *Optical Engineering* **25**, 964-969.

ONG, S.P. (1965) Light element analysis with an electron microprobe. *In* Advances in X-ray Analysis **8**. Plenum Press, New York, N.Y. (341-351).

POTTS, P.J. & TINDLE, A.G. (1989): Analytical characteristics of multilayer dispersion element ($2d = 60$ Å) in the determination of fluorine in minerals by electron microprobe. *Mineral. Mag.* **53**, 357-362.

POUCHOU, J.L & PICHOIR, F. (1991): Quantitative analysis of homogeneous or stratified microvolumes applying the model "PAP." *In* Electron Probe Quantitation (K.F.J. Heinrich & D.E. Newbury, eds.). Plenum Press, New York, N.Y. (31-75).

REED, S.J.B. (1989): Ion microprobe analysis – a review of geological applications. *Mineral. Mag.* **53**, 3-24.

———— (1993): *Electron Microprobe Analysis* (2nd ed.). Cambridge University Press, Cambridge, U.K.

SENTNER, D.A. & HEITUR, H.I. (1987): Electron probe microanalysis of Be in Cu–Be alloys with the use of a layered synthetic microstructure dispersion element. *In* Microbeam Analysis (R.H. Geiss, ed.). San Francisco Press, Inc., San Francisco, California (65-68).

SHIRAIWA, T., FUJINO, N. & MURAYAMA, J. (1972): Quantitative electron probe microanalysis of carbon and *In* Proc. 6th Int. Conf. on X-ray Optics and Microanalysis (G. Shinoda, K. Kohra & T. Ichinokawa, eds.). Univ. of Tokyo Press, Tokyo, Japan (213-218).

SOLBERG, T.N. (1982): Fluorine electron microprobe analysis: variations of X-ray peak shape. *In* Microbeam Analysis (K.F.J. Heinrich, ed.). San Francisco Press, Inc., San Francisco, California (148-150).

STORMER, J.C., JR., PIERSON, M.L. & TACKER, R.C. (1993): Variation of F and Cl X-ray intensity due to anisotropic diffusion in apatite during electron microprobe analysis. *Am. Mineral.* **78**, 641-648.

WALDO, R.A. (1991): A characteristic X-ray fluorescence correction for thin-film analysis by electron microprobe. *In* Microbeam Analysis (D.G. Howitt, ed.). San Francisco Press, Inc., San Francisco, California (45-53).

WIECH, G. (1981): X-ray emission spectroscopy. *In* Emission and Scattering Techniques. Proc. NATO Adv. Study Inst. (P. Day, ed.). D. Reidel Publishing Co., Dordrecht, The Netherlands (103-151).

WILSON, P.N., PARRY, W.T. & NASH, W.P. (1992): Characterization of hydrothermal tobelitic veins from black shale, Oquirrh Mountains, Utah. *Clays Clay Minerals* **40**, 405-420.